


# Detecting chimeras by eigenvalue decomposition of the bivariate local order parameter

FATEMEH PARASTESH<sup>1</sup>, HAMED AZARNOUSH<sup>1</sup>, SAJAD JAFARI<sup>2,1(a)</sup> and MATJAŽ PERC<sup>3,4,5</sup> 

<sup>1</sup> Department of Biomedical Engineering, Amirkabir University of Technology - No. 350, Hafez Ave, Valiasr Square, Tehran 159163-4311, Iran

<sup>2</sup> Health Technology Research Institute, Amirkabir University of Technology - No. 350, Hafez Ave, Valiasr Square, Tehran 159163-4311, Iran

<sup>3</sup> Faculty of Natural Sciences and Mathematics, University of Maribor - Koroška cesta 160, 2000 Maribor, Slovenia

<sup>4</sup> Department of Medical Research, China Medical University Hospital, China Medical University - Taichung, Taiwan

<sup>5</sup> Complexity Science Hub Vienna - Josefstädterstraße 39, 1080 Vienna, Austria

received 16 March 2020; accepted in final form 4 May 2020

published online 22 May 2020

PACS 89.75.-k – Complex systems

PACS 05.45.Xt – Synchronization; coupled oscillators

**Abstract** – It has been shown that the eigenvalue decomposition of the matrix of the bivariate phase synchronization measure can be used for the detection of cluster synchronization. It has also been shown that other measures, such as the strength of incoherence and various local order parameters, can be used to quantitatively characterize chimeras, or chimera states. Here we bridge these two domains by showing that the eigenvalue decomposition method can also be used for the detection of chimeras. We compute the local order parameter for all oscillator pairs and apply the eigenvalue decomposition on the bivariate matrix. We show that, in contrast to cluster synchronization, there are more eigenvalues above one than the number of synchronized clusters in the network. The corresponding eigenvectors correspond to synchronized groups, while the oscillators that are not represented by the eigenvectors form the chimeras. We demonstrate our approach on coupled Liénard equations and FitzHugh-Nagumo neurons.

Copyright © EPLA, 2020

**Introduction.** – Network science has attained a great interest in recent years due to its broad applicability across the social and natural sciences [1–8]. Various properties of complex networks facilitate the observation of different emergent phenomena [9–11], one of such are the chimera states [12]. The chimera state is a symmetry-breaking state, consisting of synchronized and asynchronized oscillators in an ensemble of coupled oscillators. The coexistence of coherence and incoherence was firstly observed in a network of coupled identical phase oscillators [13], and was later named “chimera” in reference to the namesake in Greek mythology [14]. After their discovery, chimeras have been investigated in a variety of coupled oscillators, including phase oscillators, periodic and chaotic systems in continuous or discrete forms, and also in different fields such as in chemical, mechanical, and biological systems [15–18]. Experimentally, chimeras have

been observed in optoelectronic oscillators [19], electrochemical oscillators [20], and coupled pendula [21,22].

A real phenomenon which is the closest to the chimera state is the uni-hemispheric sleep, observed in some aquatic mammals and birds [12]. During this sleep, in which one eye is open, one half of the brain is awake and asynchronous, while the other half is asleep and synchronous. In addition, the coexistence of synchrony and asynchrony is observed in pathological brain diseases such as Parkinson’s disease, epileptic seizures, and Alzheimer’s disease [12]. Therefore, the study of the chimera states in neuronal networks has attracted considerable attention [23–26]. Bera *et al.* [27] considered a network of bursting neurons with chemical synapses and observed chimera and multi-chimera states. Tang *et al.* [28] studied a noisy small-world network of neurons with delayed connections. They investigated the effect of noise and delay on the transient or permanent chimera states. Tian *et al.* [29] found that the electromagnetic field can induce the chimera state

<sup>(a)</sup> E-mail: sajadjafari83@gmail.com

in the neuronal network. Zakharova *et al.* [30] investigated a noisy network of coupled FitzHugh-Nagumo neurons and reported that, in the noisy network, two phenomena of coherence-resonance and chimera states emerge. In another research [31], they provided a complete analysis for the observed coherence-resonance chimeras and stated that, by tuning the intensity of noise, the size of the incoherent part of the chimera is adjustable. Furthermore, in 2017, they presented a time-delayed feedback control scheme for defining the range of parameter values at which the coherence-resonance chimeras appear [32]. Very recently, Majhi *et al.* [12] presented a comprehensive review of the studies of the chimera states in the neuronal networks.

Recent studies about chimera states have considered different network topologies and connections [33,34]. The first observation of the chimera state was in a ring of non-locally coupled oscillators [13]. Further researches revealed the emergence of chimera states for local and global couplings [35,36]. With the development of the complex networks, the chimeras were investigated in more complex frameworks [37]. These researches showed that the topology of the networks remarkably influences the formation of the chimera states. Mishra *et al.* [38] represented the existence of different chimera-like states in globally coupled networks with attractive and repulsive mean-field feedback. Argyropoulos *et al.* [39] investigated the effect of the fractal connectivity in a two-dimensional network of leaky integrate-and-fire neurons. Ulonska *et al.* [40] studied the networks of Van der Pol oscillators with hierarchical coupling topology. By computing the network clustering coefficient, they revealed that there is a relation between the level of the hierarchy and the pattern of the emergent chimera states. There are also several researches focusing on more complex structures such as multilayer or multiplex networks [41–44], as well as the time-varying connectivities [34,45].

The variety of studies on the chimera states has resulted in finding diverse patterns. These different types of chimeras are named according to the properties of the spatiotemporal patterns. Overall, if the positions of the coherent and incoherent groups are static in time, the pattern is stationary. Amplitude chimeras, phase chimeras [46], imperfect chimeras [47], multi-headed chimeras [48], and chimera death [49] are some examples of the stationary chimera states. When the coherent and incoherent groups change their positions in time, the non-stationary chimera is formed. For instance, alternating chimeras [50] and traveling chimeras [51] belong to the non-stationary chimera states. Indeed, the identification of these patterns needs proper analytical measures.

Several analytical methods have been used for the characterization of the chimera states. The local order parameter, the strength of incoherence, Lyapunov spectrum analysis, and mean phase velocity are some of the measures used for quantification of the chimera states [12,52]. In this paper, we show that the eigenvalue

decomposition can be used to characterize the chimera states and detect the positions of synchronized and asynchronized oscillators precisely. In 2005, Müller *et al.* [53] showed that the level of synchronization of the multivariate time series is related to the highest and lowest eigenvalues of the correlation matrix. In 2007, Allefeld *et al.* [54] demonstrated the utility of eigenvalue decomposition of the matrix of indices of bivariate phase synchronization strength in detecting the cluster synchronization, in which the network splits into clusters of synchronized oscillators. Here, firstly, we compute the local order parameter for all the pairs of the oscillators of the network that exhibit chimera state and obtain the matrix of the bivariate local order parameter. Then we calculate the eigenvalues and eigenvectors of this matrix and show that it is possible to find the synchronized oscillators. We propose an algorithm that defines whether all of the oscillators are located in the synchronized groups or not. If there are some oscillators that are not in any synchronized cluster, the state of the network is the chimera. In summary, the advantages of this method are: 1) detecting the chimera state from the synchronized and asynchronized states, 2) distinguishing the multi-chimera state from the ordinary chimera state, 3) identifying the exact location of the synchronized and asynchronized oscillators. Therefore, the non-adjacent synchronous oscillators can also be determined, while the other methods, such as the local order parameter and the strength of incoherence, consider only the neighboring oscillators. It is notable that the used bivariate local order parameter is averaged in time, and therefore, it can just define the stationary chimeras.

**Method.** – A dynamical network consisting of coupled nonlinear oscillators can be described by

$$\frac{dx_i}{dt} = F(x_i) - \sigma \sum_{j=1}^N G_{ij} H(x_j), \quad (1)$$

where  $x_i$  is a  $d$ -dimensional vector,  $F(x_i)$  is the dynamics of the isolated oscillator,  $H(x)$  is the coupling function,  $\sigma$  is the coupling strength,  $G$  is the coupling matrix, and  $N$  is the network size. The network may exhibit different synchronous patterns by varying the parameters. In special parameter values, the chimera state may be observed. For characterizing the behavior of the network, several order parameters have been used [55,56]. To specify the coherent and incoherent parts of the chimera states, a local order parameter [52] is often used as

$$Z_k = \left| \frac{1}{2\delta} \sum_{|j-k| \leq \delta} e^{i\theta_k} \right|, \quad k = 1, 2, \dots, N, \quad (2)$$

where  $\theta_k$  denotes the geometric phase of the  $j$ -th oscillator, and  $\delta$  is the size of the considered neighbors. Consequently, the local order parameter  $Z_k = 1$  shows that the  $k$ -th unit belongs to the coherent part of the chimera state, and  $Z_k < 1$  refers to the incoherent parts. Here, to have a matrix of bivariate dependencies, we compute the

local order parameter for all of the pairs of oscillators as

$$Z_{jk} = \left\langle \left| \frac{1}{2}(e^{i\theta_k} + e^{i\theta_j}) \right| \right\rangle_t, \quad j, k = 1, 2, \dots, N. \quad (3)$$

Similarly,  $Z_{jk} = 1$  indicates that the  $j$ -th and  $k$ -th oscillators are coherent, and  $Z_{jk} < 1$  shows incoherency. To calculate the eigenvalues of the bivariate local order matrix, firstly, we convert this matrix to a binary matrix, where 1 denotes the coherency, and 0 denotes the incoherency between oscillators. Thus, we compute the Heaviside function of the matrix  $Z$  as  $L = \text{Heaviside}(Z - 1 + \epsilon)$ , where  $\epsilon$  is a small threshold fixed at  $\epsilon = 0.01$ . Then, we apply the eigenvalue decomposition on the binary local order parameter matrix ( $L$ ). The binary local order parameter matrix has the properties of the correlation matrix discussed in [52], *i.e.*, the eigenvalues of  $L$  are non-negative, and the eigenvalues and the eigenvectors are real-valued, and  $\sum \lambda_k = \text{tr}(L) = N$ . In the case of a completely incoherent network, only the diagonals of  $L$  are equal to 1, and other elements are zero. Therefore, all of the eigenvalues are equal to 1. When there is some coherency between some oscillators, some elements of  $L$  which relate to the coherent oscillators change to 1. Subsequently, the eigenvalues are changed such that some of them become greater than 1. In this case, the eigenvectors relating to the eigenvalues above 1 represent the coherent oscillators.

#### Chimera state in coupled Liénard equations. –

In [38], the authors have shown that the network of coupled Liénard equations exhibits different dynamical behaviors such as cluster synchronization and chimera state. The network of  $N$  identical Liénard equations can be described by

$$\begin{aligned} \dot{x}_i &= y_i, \\ \dot{y}_i &= -\alpha x_i y_i - \beta x_i^3 - \gamma x_i + \sigma[(\bar{y} - y_i) + \varepsilon(\bar{x} - x_i)], \end{aligned} \quad (4)$$

where  $\alpha = 0.45$ ,  $\beta = 0.5$ ,  $\gamma = -0.5$ ,  $N = 100$ , and  $\bar{x} = \frac{1}{N} \sum_{i=1}^N x_i$ ,  $\bar{y} = \frac{1}{N} \sum_{i=1}^N y_i$ . For the numerical investigation of the eigenvalue decomposition, we start with the case of cluster synchronization. Figure 1(a) shows the spatiotemporal pattern of the Liénard network for  $\sigma = 1.7$  and  $\varepsilon = -0.09$ . In this case, the network splits into two synchronized clusters. Figure 1(b) depicts the time snapshot of this pattern and fig. 1(c) shows the local order matrix  $L$ . The eigenvalue decomposition of matrix  $L$  shows that this matrix has two eigenvalues above 1 (fig. 1(d)), whose corresponding eigenvectors are shown in fig. 1(e). These eigenvectors clearly show the positions of the synchronized oscillators. From the spatiotemporal pattern, it seems that the two clusters have different attractors. To depict these attractors, the phase space of two oscillators of different clusters, together with the nullclines of the Liénard system are illustrated in fig. 1(f). It is observed that in these parameters, both attractors are periodic.

Next, the parameters are set at  $\sigma = 1.6$  and  $\varepsilon = -1.8$ , at which the network consists of synchronized and

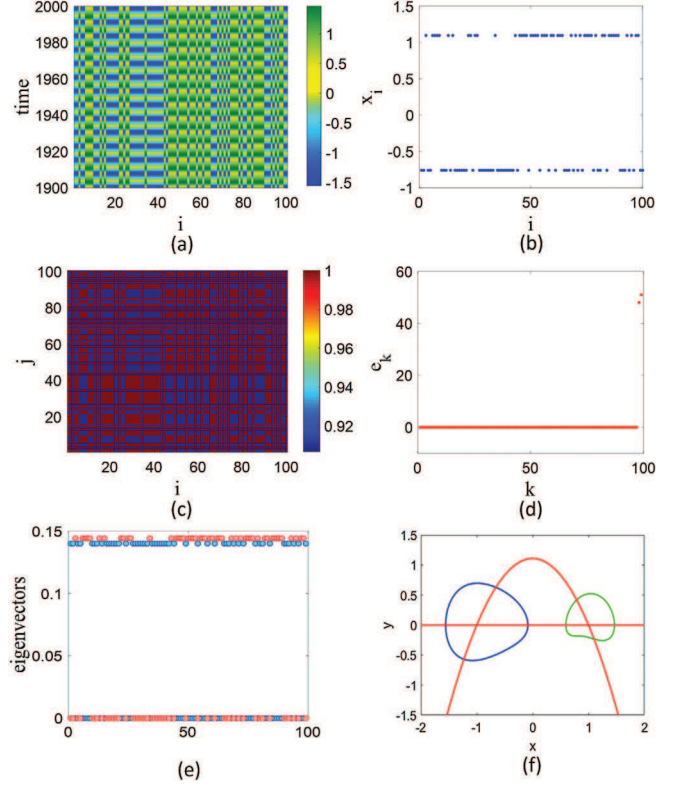


Fig. 1: The coupled Liénard equations in  $\sigma = 1.7$  and  $\varepsilon = -0.09$  exhibiting cluster synchronization. Panel (a) shows the spatiotemporal pattern of the  $x$  variables of the oscillators. The time snapshot of  $x$  variables at  $t = 2000$  is illustrated in panel (b). In this figure, the dependency of the oscillators on two clusters is clear. Panel (c) shows the matrix of the bivariate local order parameter of the network, whose eigenvalues are shown in panel (d). Panel (e) shows the two eigenvectors corresponding to the eigenvalues above 1. The eigenvectors show that all of the oscillators belong to synchronized clusters. In panel (f), the phase space of two clusters (blue and green), and the nullclines of the Liénard system (red) are shown.

asynchronized clusters, and thus the pattern is chimera state. Figures 2(a), (b) depict the spatiotemporal pattern and the time snapshot of the network in this case. The local order matrix of this state is illustrated in fig. 2(c) and its eigenvalues are shown in fig. 2(d). It is observed that there are two eigenvalues above 1, whose eigenvectors are shown in fig. 2(e). The first eigenvector (blue) shows the oscillators belonging to the larger synchronized cluster, and the second one (red) shows that three of the other oscillators are also synchronized. The rest of the oscillators which are not involved in these two eigenvectors are asynchronized. As is shown in fig. 2(f), with these parameters, the oscillators are attracted by two chaotic attractors. In order to specify the behavior of the network and whether the state is chimera or cluster synchronization, the following algorithm is proposed:

- 1) Sum the eigenvectors which correspond to the eigenvalues above 1:  $V = \sum |v_k|$ .

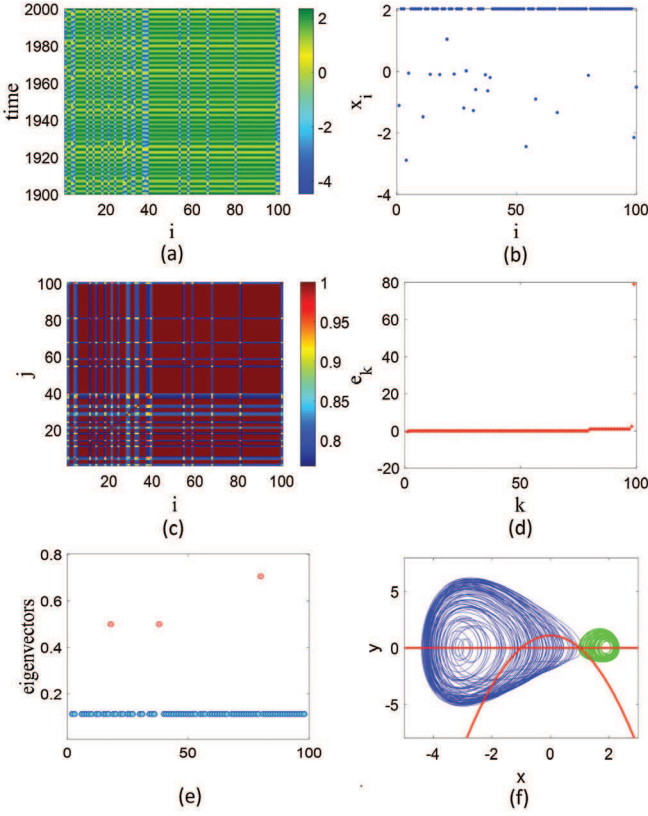


Fig. 2: The coupled Liénard equations in  $\sigma = 1.6$  and  $\varepsilon = -1.8$  exhibiting chimera state. Panel (a) shows the spatiotemporal pattern of the  $x$  variables of the oscillators, and panel (b) shows the time snapshot of  $x$  variables at  $t = 2000$ . Panel (c) illustrates the matrix of the bivariate local order parameter of the network, and its eigenvalues are depicted in panel (d). Panel (e) shows the two eigenvectors corresponding to the eigenvalues above 1. The eigenvectors show that some of the oscillators do not belong to the synchronized clusters, and therefore the pattern is chimera state. The two chaotic attractors of the oscillators (blue and green), and the nullclines of the Liénard system (red) are shown in panel (f).

- 2) Apply the sign function on the sum of eigenvectors:  $S = \text{sign}(V)$ . This function assigns the value one to the oscillators, which belong to a synchronized cluster, and assigns zero to the asynchronous ones.
- 3) Sum the signed vector ( $S$ ):  $C = \sum_{i=1}^N S_i$ . Thus the value  $C = 0$  shows that the oscillators are asynchronous, while  $C = N$  represents that all of the oscillators belong to synchronized groups. Finally,  $0 < C < N$  represents chimera state such that the  $C$  of the oscillators belong to the synchronized clusters and  $N - C$  of them construct the asynchronous group.

For the network shown in fig. 2, the value of  $C$  is equal to 82, which confirms the chimera state.

**Multi-chimera states in coupled FitzHugh-Nagumo neurons.** – The network of coupled FitzHugh-Nagumo neurons has been investigated in many chimera

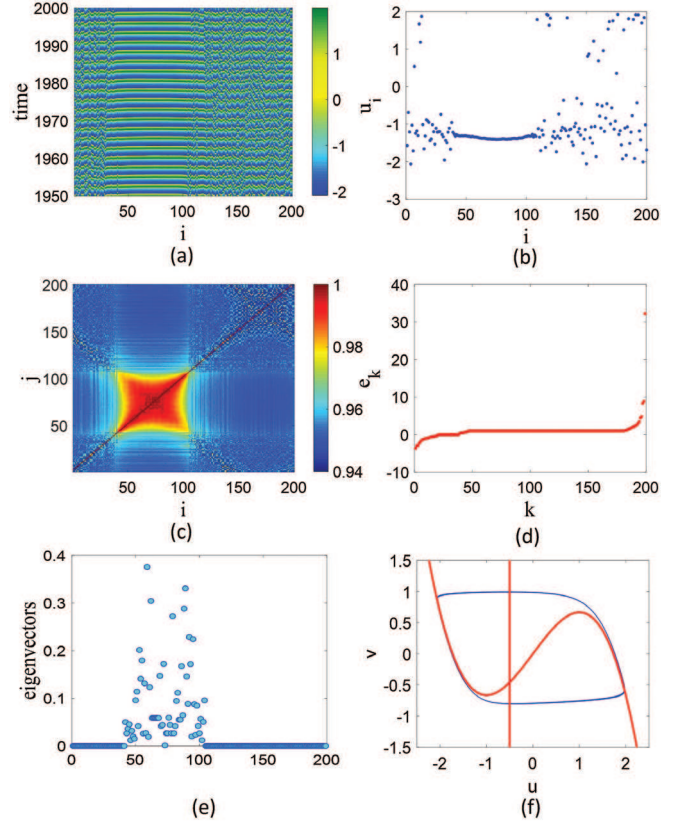


Fig. 3: The coupled FitzHugh-Nagumo neurons in  $\sigma = 0.1$  and  $r = 0.35$  exhibiting chimera state. Panel (a) shows the spatiotemporal pattern of the  $u$  variables of the oscillators, and panel (b) shows the time snapshot of  $u$  variables at  $t = 2000$ . The matrix of the bivariate local order parameter  $L$  of the network is illustrated in panel (c), and its eigenvalues are depicted in panel (d). Panel (e) shows one eigenvector corresponding to eigenvalues above 1, which represents the position of synchronized oscillators. Panel (f) illustrates the phase space of the oscillators and the nullclines of the FitzHugh-Nagumo system.

studies [25,31,57]. The dynamical equations of this network are described by

$$\begin{aligned} \varepsilon \dot{u}_i &= u_i - \frac{u_i^3}{3} - v_i + \frac{\sigma}{2R} \sum_{j=i-R}^{j=i+R} [b_{uu}(u_j - u_i) \\ &\quad + b_{uv}(v_j - v_i)], \\ \dot{v}_i &= u_i + a + \frac{\sigma}{2R} \sum_{j=i-R}^{j=i+R} [b_{vu}(u_j - u_i) \\ &\quad + b_{vv}(v_j - v_i)], \end{aligned} \quad (5)$$

where  $u_i$  and  $v_i$  are the activator and inhibitor variables, and  $\varepsilon = 0.05$  is a small parameter characterizing a timescale separation. The parameter  $a$  determines the local dynamics of the oscillators and is set at  $a = 0.5$ .  $\sigma$  is the coupling strength, and the coupling is considered to be nonlocal, such that each oscillator is coupled to its  $2R$  nearest neighbors. The coefficients of the direct and



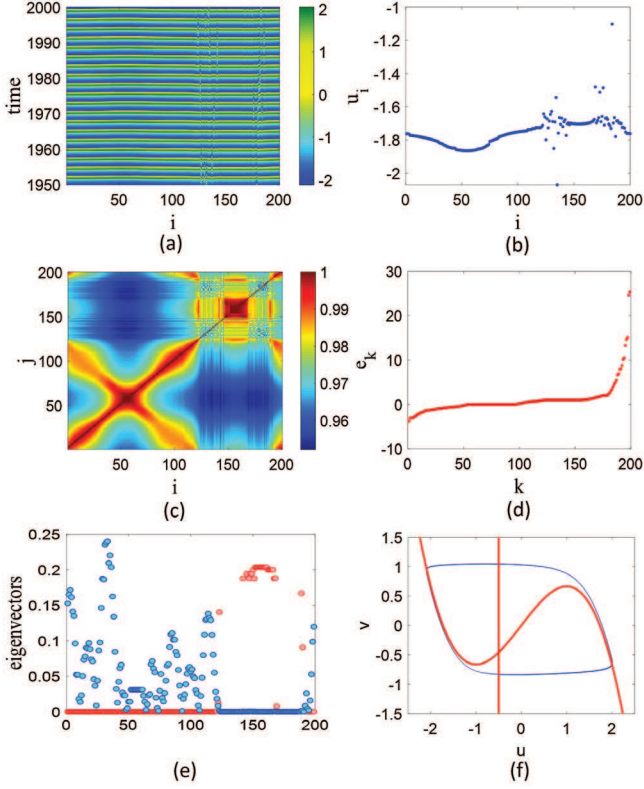


Fig. 4: The coupled FitzHugh-Nagumo neurons in  $\sigma = 0.28$  and  $r = 0.33$  exhibiting a 2-headed multi-chimera state. Panel (a) shows the spatiotemporal pattern of the  $u$  variables of the oscillators, and panel (b) shows the time snapshot of  $u$  variables at  $t = 2000$ , wherein two synchronized clusters are observed. The matrix of the bivariate local order parameter  $L$  of the network is illustrated in panel (c), and its eigenvalues are depicted in panel (d). Panel (e) shows the eigenvectors, defining two synchronized clusters. Panel (f) illustrates the phase space of the oscillators and the nullclines of the FitzHugh-Nagumo system.

cross-couplings are determined by

$$B = \begin{pmatrix} b_{uu} & b_{uv} \\ b_{vu} & b_{vv} \end{pmatrix} = \begin{pmatrix} \cos \phi & \sin \phi \\ -\sin \phi & \cos \phi \end{pmatrix}, \quad (6)$$

where  $\phi = \pi/2 - 0.1$  is fixed. By varying the coupling parameters,  $\sigma$ , and  $R$ , this network is capable of exhibiting different chimera and multi-chimera states.

By setting  $\sigma = 0.1$  and  $r = R/N = 0.35$ , the network shows the chimera state. Figures 3(a), (b) illustrate the spatiotemporal pattern and the time snapshot of the network in this case. As the figures show, there is one coherent group of oscillators in the network. The computed local order matrix of the network is shown in fig. 3(c) and its eigenvalues are illustrated in fig. 3(d). It is observed that a large number of eigenvalues are above 1. But not all the corresponding eigenvectors show distinct synchronized clusters. Actually, some of the eigenvectors are repetitive and determine one synchronized cluster. Figure 3(e) shows the eigenvector specifying the coherent

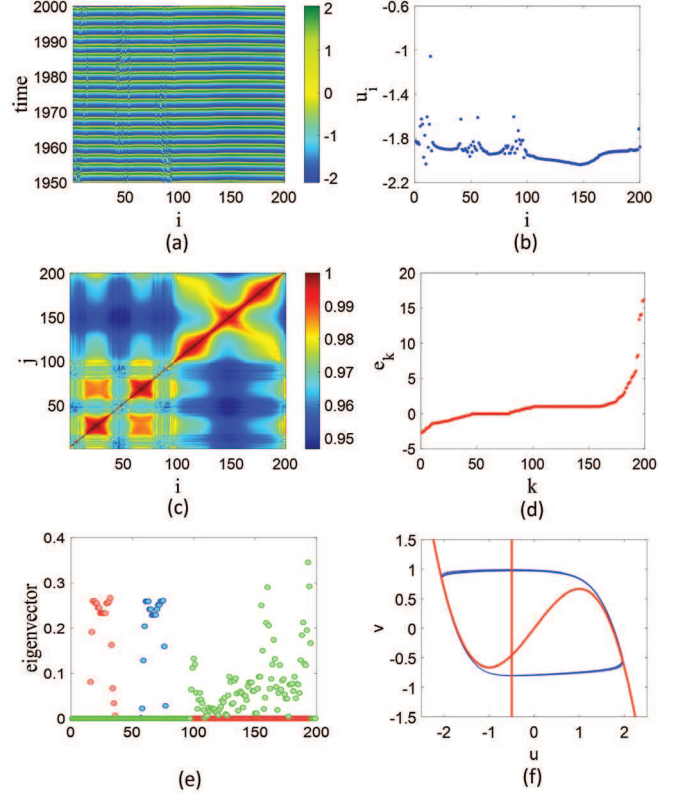


Fig. 5: The coupled FitzHugh-Nagumo neurons in  $\sigma = 0.25$  and  $r = 0.25$  exhibiting a 3-headed multi-chimera state. Panel (a) shows the spatiotemporal pattern of the  $u$  variables of the oscillators, and panel (b) shows the time snapshot of  $u$  variables at  $t = 2000$ , wherein three synchronized clusters are obvious. The matrix of the bivariate local order parameter  $L$  of the network is illustrated in panel (c), and its eigenvalues are depicted in panel (d). Panel (e) shows the eigenvectors, defining three synchronized clusters. Panel (f) illustrates the phase space of the oscillators and the nullclines of the FitzHugh-Nagumo system.

oscillators. The number of synchronized oscillators for this pattern is  $C = 65$ . In contrast to the Liénard network, in this network, all of the oscillators have the same periodic attractor. Figure 3(f) shows the phase space of oscillators (blue) and the nullclines (red) of the FitzHugh-Nagumo system.

By strengthening the coupling strength, the multi-chimera states emerge, in which there is more than one incoherent group. Figures 4(a), (b) show the spatiotemporal pattern and the snapshot of the network for  $\sigma = 0.28$  and  $r = 0.33$ . In this case, the network is composed of two incoherent and two coherent groups. The local order matrix of the network is illustrated in fig. 4(c) and its eigenvalues are depicted in fig. 4(d). The eigenvectors indicating the coherent groups are represented in fig. 4(e). According to the eigenvectors, there are two synchronized clusters. However, all of the oscillators have the same attractor, which is shown in fig. 4(f). In this case, we have  $C = 158$ .

Finally, we examine a 3-headed multi-chimera state. Figure 5 shows the network pattern and eigenvalue decomposition results for  $\sigma = 0.25$  and  $r = 0.25$  at which three synchronized clusters exist. In fig. 5(e), the three eigenvectors which show three synchronized clusters are illustrated. Therefore, the eigenvectors can indicate the synchronized clusters as well. In this case, the value of  $C$  is 140. Similar to the chimera state and 2-headed chimera state, all of the oscillators have the same periodic attractor, as shown in fig. 5(f).

**Conclusions.** – In 2005, Müller *et al.* [53] used the method of eigenvalue decomposition of the correlation matrix for analyzing the correlation of the multivariate time series. In 2007, Allefeld *et al.* [54] demonstrated that the eigenvalue decomposition of the matrix of bivariate phase synchronization strength can be applied for detecting the cluster synchronization. The aim of this paper was to show that the eigenvalue decomposition is also utilizable in finding the chimera state. One of the characteristic measures used in the chimera studies is the local order parameter. Here, we considered the networks exhibiting chimera state and multi-chimera state, and computed the local order parameter for all the pairs of the oscillators. We obtained the bivariate local order matrix, wherein the elements equal to one show the synchronized pairs, and the elements lower than one represent the asynchronized ones. In the case of  $M$ -cluster synchronization, the eigenvalue decomposition results in  $M$  eigenvalues greater than one, where the corresponding eigenvectors represent the synchronized clusters. But in the eigenvalue decomposition of the bivariate local order parameter matrix in the case of chimera state, the number of the eigenvalues greater than one was more than the number of the synchronized clusters. However, some of the eigenvectors were repetitive and indicated the same synchronized clusters. Overall, these eigenvectors could show the synchronized oscillators, and the other oscillators, which were not in the synchronized clusters, formed the asynchronized group of chimera. We examined different examples of chimera states, including simple chimera states, 2-headed chimeras, and 3-headed chimeras. We have also investigated the larger network with  $N = 1000$  and obtained the same results. Therefore, this method is not dependent on the network size. Our results show that the eigenvalue decomposition can detect all of these patterns, and thus we recommend it favorably for applications in other systems.

\*\*\*

MP was supported by the Slovenian Research Agency (Grant Nos. J4-9302, J1-9112, and P1-0403).

## REFERENCES

- [1] ALBERT R. and BARABÁSI A.-L., *Rev. Mod. Phys.*, **74** (2002) 47.
- [2] BOCCALETTI S., LATORA V., MORENO Y., CHAVEZ M. and HWANG D., *Phys. Rep.*, **424** (2006) 175.
- [3] DOROGOVTSSEV S. N., GOLTSEV A. V. and MENDES J. F. F., *Rev. Mod. Phys.*, **80** (2008) 1275.
- [4] FORTUNATO S., *Phys. Rep.*, **486** (2010) 75.
- [5] BARTHÉLEMY M., *Phys. Rep.*, **499** (2011) 1.
- [6] HOLME P. and SARAMÄKI J., *Phys. Rep.*, **519** (2012) 97.
- [7] BOCCALETTI S., BIANCONI G., CRIADO R., DEL GENIO C., GÓMEZ-GARDEÑES J., ROMANCE M., SENDIÑA-NADAL I., WANG Z. and ZANIN M., *Phys. Rep.*, **544** (2014) 1.
- [8] KIVELÄ M., ARENAS A., BARTHELEMY M., GLEESON J. P., MORENO Y. and PORTER M. A., *J. Complex Netw.*, **2** (2014) 203.
- [9] LI H.-J., BU Z., WANG Z. and CAO J., *IEEE Trans. Ind. Inform.*, **16** (2019) 5327.
- [10] LI H.-J., WANG Q., LIU S. and HU J., *Physica A*, **542** (2020) 123514.
- [11] NEPOMUCENO E. G. and PERC M., *J. Complex Netw.*, **8** (2020) cnz015.
- [12] MAJHI S., BERA B. K., GHOSH D. and PERC M., *Phys. Life Rev.*, **28** (2019) 100.
- [13] KURAMOTO Y. and BATTOGTOKH D., *Nonlinear Phenom. Complex Syst.*, **5** (2002) 380.
- [14] ABRAMS D. M. and STROGATZ S. H., *Phys. Rev. Lett.*, **93** (2004) 174102.
- [15] DUDKOWSKI D., CZOLCZYŃSKI K. and KAPITANIAK T., *Nonlinear Dyn.*, **95** (2019) 1859.
- [16] FAGHANI Z., ARAB Z., PARASTESH F., JAFARI S., PERC M. and SLAVINEC M., *Chaos, Solitons Fractals*, **114** (2018) 306.
- [17] VADIVASOVA T. E., STRELKOVA G. I., BOGOMOLOV S. A. and ANISHCHENKO V. S., *Chaos*, **26** (2016) 093108.
- [18] TINSLEY M. R., NKOMO S. and SHOWALTER K., *Nat. Phys.*, **8** (2012) 662.
- [19] HART J. D., BANSAL K., MURPHY T. E. and ROY R., *Chaos*, **26** (2016) 094801.
- [20] WICKRAMASINGHE M. and KISS I. Z., *Phys. Chem. Chem. Phys.*, **16** (2014) 18360.
- [21] DUDKOWSKI D., GRABSKI J., WOJEWODA J., PERLIKOWSKI P., MAISTRENKO Y. and KAPITANIAK T., *Sci. Rep.*, **6** (2016) 29833.
- [22] WOJEWODA J., CZOLCZYŃSKI K., MAISTRENKO Y. and KAPITANIAK T., *Sci. Rep.*, **6** (2016) 34329.
- [23] CALIM A., HÖVEL P., OZER M. and UZUNTARLA M., *Phys. Rev. E*, **98** (2018) 062217.
- [24] PARASTESH F., JAFARI S., AZARNOUSH H., HATEF B., NAMAZI H. and DUDKOWSKI D., *Eur. Phys. J. ST*, **228** (2019) 2023.
- [25] SHEPELEV I. A., VADIVASOVA T. E., BUKH A., STRELKOVA G. and ANISHCHENKO V., *Phys. Lett. A*, **381** (2017) 1398.
- [26] WEI Z., PARASTESH F., AZARNOUSH H., JAFARI S., GHOSH D., PERC M. and SLAVINEC M., *EPL*, **123** (2018) 48003.
- [27] BERA B. K., GHOSH D. and LAKSHMANAN M., *Phys. Rev. E*, **93** (2016) 012205.
- [28] TANG J., ZHANG J., MA J. and LUO J., *Sci. China Technol. Sci.*, **62** (2019) 1134.
- [29] TIAN C., CAO L., BI H., XU K. and LIU Z., *Nonlinear Dyn.*, **93** (2018) 1695.

- [30] ZAKHAROVA A., SEMENOVA N., ANISHCHENKO V. and SCHÖLL E., in *International Conference on Patterns of Dynamics* (Springer) 2016, pp. 44–63.
- [31] SEMENOVA N., ZAKHAROVA A., ANISHCHENKO V. and SCHÖLL E., *Phys. Rev. Lett.*, **117** (2016) 014102.
- [32] ZAKHAROVA A., SEMENOVA N., ANISHCHENKO V. and SCHÖLL E., *Chaos*, **27** (2017) 114320.
- [33] BERA B. K., MAJHI S., GHOSH D. and PERC M., *EPL*, **118** (2017) 10001.
- [34] BUSCARINO A., FRASCA M., GAMBUTTA L. V. and HÖVEL P., *Phys. Rev. E*, **91** (2015) 022817.
- [35] LAING C. R., *Phys. Rev. E*, **92** (2015) 050904.
- [36] YELDESBAI A., PIKOVSKY A. and ROSENBLUM M., *Phys. Rev. Lett.*, **112** (2014) 144103.
- [37] ZHU Y., ZHENG Z. and YANG J., *Phys. Rev. E*, **89** (2014) 022914.
- [38] MISHRA A., HENS C., BOSE M., ROY P. K. and DANA S. K., *Phys. Rev. E*, **92** (2015) 062920.
- [39] ARGYROPOULOS G., KASIMATIS T. and PROVATA A., *Phys. Rev. E*, **99** (2019) 022208.
- [40] ULONSKA S., OMELCHENKO I., ZAKHAROVA A. and SCHÖLL E., *Chaos*, **26** (2016) 094825.
- [41] MAJHI S., PERC M. and GHOSH D., *Chaos*, **27** (2017) 073109.
- [42] KASATKIN D., YANCHUK S., SCHÖLL E. and NEKORKIN V., *Phys. Rev. E*, **96** (2017) 062211.
- [43] MAKSIMENKO V. A., MAKAROV V. V., BERA B. K., GHOSH D., DANA S. K., GOREMYKO M. V., FROLOV N. S., KORONOVSKII A. A. and HRAMOV A. E., *Phys. Rev. E*, **94** (2016) 052205.
- [44] MIKHAYLENKO M., RAMLOW L., JALAN S. and ZAKHAROVA A., *Chaos*, **29** (2019) 023122.
- [45] SANTOS M. S., PROTACHEVICZ P. R., IAROSZ K. C., CALDAS I. L., VIANA R. L., BORGES F. S., REN H.-P., SZEZECZ J. D. jr., BATISTA A. M. and GREBOGI C., *Chaos*, **29** (2019) 043106.
- [46] BOGOMOLOV S. A., SLEPNEV A. V., STRELKOVA G. I., SCHÖLL E. and ANISHCHENKO V. S., *Commun. Nonlinear Sci. Numer. Simulat.*, **43** (2017) 25.
- [47] PARASTESH F., JAFARI S., AZARNOUSH H., HATEF B. and BOUNTIS A., *Chaos, Solitons Fractals*, **110** (2018) 203.
- [48] JAROS P., BORKOWSKI L., WITKOWSKI B., CZOLCZYNSKI K. and KAPITANIAK T., *Eur. Phys. J. ST*, **224** (2015) 1605.
- [49] ZAKHAROVA A., KAPPELLER M. and SCHÖLL E., *Phys. Rev. Lett.*, **112** (2014) 154101.
- [50] MAJHI S. and GHOSH D., *Chaos*, **28** (2018) 083113.
- [51] MISHRA A., SAHA S., GHOSH D., OSIPOV G. V. and DANA S. K., *Opera Med. Physiol.*, **3** (2017) 14.
- [52] WOLFRUM M., OMEL'CHENKO O. E., YANCHUK S. and MAISTRENKO Y. L., *Chaos*, **21** (2011) 013112.
- [53] MÜLLER M., BAIER G., GALK A., STEPHANI U. and MUHLE H., *Phys. Rev. E*, **71** (2005) 046116.
- [54] ALLEFELD C., MÜLLER M. and KURTHS J., *Int. J. Bifurcat. Chaos*, **17** (2007) 3493.
- [55] BERA B. K., *Chaos*, **29** (2019) 041104.
- [56] BERA B. K., *Chaos*, **30** (2020) 023132.
- [57] OMELCHENKO I., PROVATA A., HIZANIDIS J., SCHÖLL E. and HÖVEL P., *Phys. Rev. E*, **91** (2015) 022917.